MODELING, IDENTIFICATION AND CONTROL, 1987, VOL. 8, NO. 2, 103–115
doi:10.4173/mic.1987.2.3

Three-dimensional calculations on smelting electrodes†

REIDAR INNVAER‡, KNUT FIDJE‡ and TERJE SIRA§

Keywords: *Smelting electrode, mathematical model, Maxwell equations.*

Søderberg selfbaking electrodes are used to conduct electric current into the electric reduction furnace. Two-dimensional computer models for the computation of temperatures, electric currents and thermal stresses have been used for a long time in the R&D effort to improve the construction and operation of the electrode.

This paper presents a three-dimensional model for the temperature and electric current fields in the electrode and shows how the model is used to study effects which cannot be captured in a two-dimensional model.

Since alternating current is used in the electric reduction furnace operation, the quasi-stationary approximations of the Maxwell equations have to be solved in order to compute the current distribution. These equations are solved using the magnetic vector potential and a scalar potential as the primary variables.

1. Introduction

Søderberg selfbaking electrodes are of primary importance for large electric reduction furnaces, as they conduct high electric current into the smelting process. Three electrodes are normally arranged symmetrically supplying three-phase current into a cylindrical furnace pot. Satisfactory furnace operation depends on proper electrode performance, and since the invention of the electrode system, an extensive R&D effort has been carried out to improve the electrode carbon paste, the equipment and the operation.

During the last 20 years, mathematical models and computers have been used to calculate the distribution of electric current, temperatures and thermal stresses in electrodes, as previously reported (Olsen 1972, Innvær 1976, Innvær 1980). All these calculations were carried out in two dimensions. However, this paper goes one step further and presents a three-dimensional mathematical model, called ELKEM 3X. The model computes alternating current and temperature distributions in Søderberg electrodes under stationary conditions.

The two-dimensional models, based on cylindrical geometry, have given valuable information on most electrode parameters. For the complex electrode holder area, where electrical and thermal asymmetry easily occur, a reliable simulation can only be made in three dimensions. When this part of the electrode is studied, it is important to understand the effect of parameters such as: the electric current entering the electrode, the properties of the carbon materials, the temperatures of the cooling water, the electrical contact resistances, the design of the steel casing and the internal fins, etc. These parameters determine the success of the baking process, the

Received 14 December 1986.

† Reprinted from 43rd Electric Furnace Conference Proceedings 10–13 December, 1985 Atlanta, GA, with permission of AIME, Iron and Steel Society, Electric Furnace Division.

‡ Elkem a/s, R&D Center, Kristiansand, Norway.

§ Institute for Energy Technology, Postboks 40, 2007 Kjeller, Norway.

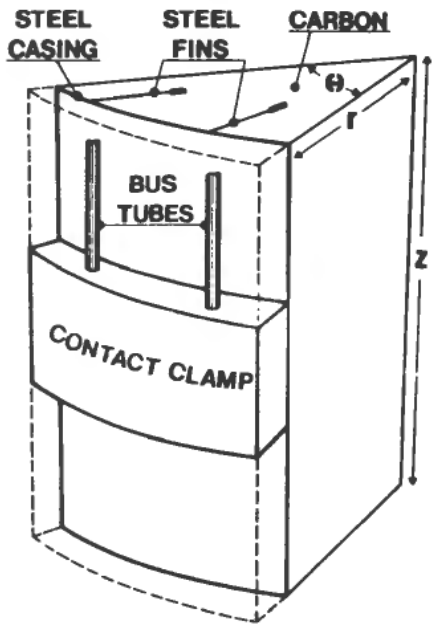

Figure 1. Segment of a Søderberg electrode for computations.

basis for the whole Søderberg system. An improved electrode is obtained when the baking is uniform along the periphery at the level of the holder. The computations have been concentrated on these items.

Furthermore, the work has simulated an electrode operating in a ferrosilicon furnace. The selected electrode diameter is 1·7 m, carrying a current of 130 kA and with a slipping rate of 0·6 m/24 h. An electrode segment, the computational domain for most of the calculations, is presented in Fig. 1. A simple sketch of the cross-sectional area of an electrode with two different holder/clamp designs is shown in Fig. 2.

2. Objectives

2.1. Operation and design

Experience with Søderberg electrodes shows that best performance is obtained under stable and continuous operational conditions. Even if this is impossible in reality, the following factors should be taken into consideration.

The current generates heat as it passes through the electrode. Some of the heat is used in the baking of the paste. Furnace shut-downs or other changes in the electrode current develop unwanted temperature gradients and corresponding thermal stresses, which may crack the baked electrode materials.

The slipping rate of the electrode is related to the electrode consumption. The baking of paste in the holder area should be a constant process. A slipping in small increments is necessary in order to avoid breakage in the soft paste.

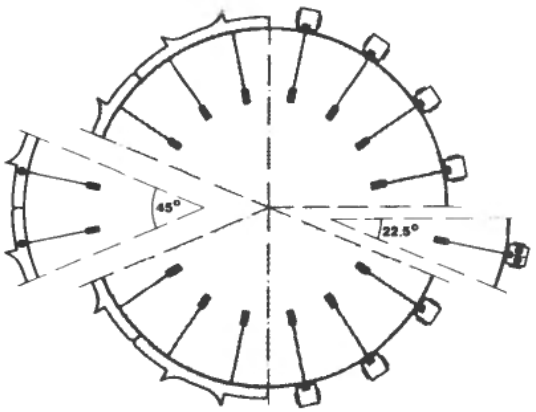

Figure 2. Cross-section of an electrode with two different holders/clamps.

The electrode movement in the furnace is performed in relation to the slipping rate, while the holder is also adjusted to the position of the electrode tip and the metallurgical conditions in the furnace process zone. Preferably, the movement should be as small as possible.

The paste charging and melting in the upper electrode part depends on temperature and pressure. A regular charging—at least once a day—should be the rule. Overheating in local parts of the soft paste should be avoided.

The steel casings in the upper electrode should be properly welded together. In order to maintain a continuous electrode column, the fins in the sections should also be welded in the joints.

All the above mentioned factors should be under strict observation during electrode operation. But even if satisfactory conditions are obtained in the 'vertical direction', the electrode will not be axisymmetrical due to the electrode design itself, as well as the electrode installation/position in the furnace pot. Some of these factors deserve further explanation.

The proximity effect, the distortion of the current in the electrode due to the current in the adjacent conductors, will have a certain influence. This has been explained previously and therefore unnecessary to include in this paper (Bøckman 1968).

The skin effect or the concentration of electric current near the surface is quite noticeable in large electrodes (Bøckman 1968). The electric current is unevenly distributed radially by the skin effect. Along the periphery, however, the effect causes no distortion of the current. The skin effect is taken care of in the mathematical equations of the model and will be demonstrated.

The surroundings will normally give a hotter electrode towards the furnace centre due to a smaller amount of heat loss. Temperature measurements carried out on the electrode surface between the holder and the charge level, show considerable differences. Similar results are found higher up in the column, both due to the surrounding temperatures and the induced eddy currents from the electric current supply.

The electrode holder, comprising the electrical and the mechanical parts as well as the electrode materials covered by these components, is a very important part of the system. It is also a very complex construction, which will be described in more detail in the following section.

2.2. Electrode holder

Figures 1 and 2 show how the current is transferred to the contact clamps in the copper bus tubes, which again are connected to the transformers. In the holder, half the clamps receive current from one transformer, while the other four clamps are connected to a second transformer. Each electrode is being fed by two transformers. This means that some current components will have a phase difference of 60 degrees, leading to unwanted current paths in the holder area.

The current enters the electrode casing from the contact clamps and is further distributed to the electrode materials. The current distribution between the clamps and casing depends strongly on the contact pressure and the electrical contact resistance—in addition to the temperatures. A high and even pressure with a clean contact surface will tend to transfer the current to the lower tip of the clamps. A layer on the clamps—for example, of baked paste which has leaked out through the casing—may cause problems for the current transfer. The importance of effective and controlled water cooling should also be pointed out. Again, the pressure and the contact surface determine the thermal conditions. The heat losses in the cooling water through the clamps give an impression of the holder conditions. An example, measurement on a 1·7 m diameter electrode, is illustrated in Fig. 3.

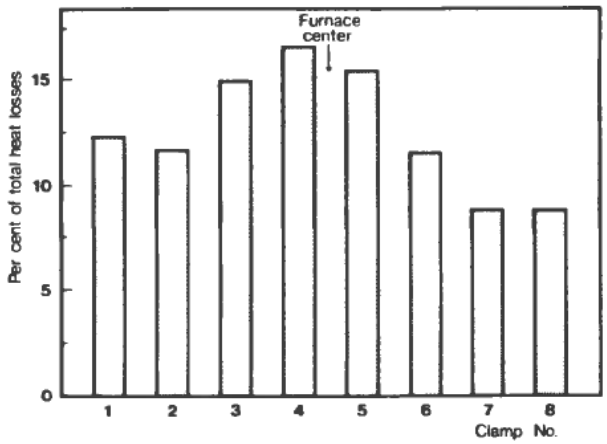

Figure 3. Heat losses in cooling water through the contact clamps.

From the outer electrode casing the current is distributed to the steel fins and the carbon materials. This is related to the electric resistance of the materials, which again depends on the dimensions and quality of the steel, and the paste used. The temperature distribution is also important for the current distribution. A negligible amount of the current is conducted in carbon before it is baked at 450° to 500°C. The contact between the steel and carbon is an uncertain factor. Due to paste shrinkage and different thermal expansions, slots between the materials may occur.

As already mentioned, the baking of the new electrode takes place in the holder area. During this process the paste properties are drastically changed by the influ-

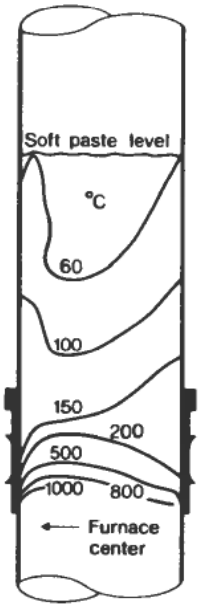

Figure 4. Measured electrode temperatures in the vertical direction.

ence of increasing temperature. Safe operation depends on good agreement between the current and the slipping. A typical temperature distribution in the vertical direction is shown in Fig. 4, measured on a 1·7 m diameter electrode in ferrosilicon production. Figure 5 illustrates temperatures in a cross-sectional area of the same electrode. If a more axisymmetrical baking zone could be obtained, the slipping rate at a constant current could be increased—if needed—and the shrinkage/expansion during the baking process will give a better electrode. In addition to improved operation, savings can be obtained by avoiding damage to holder components due to arcing, with a local current which is too high, of high local currents, optimization of the casing design, etc.

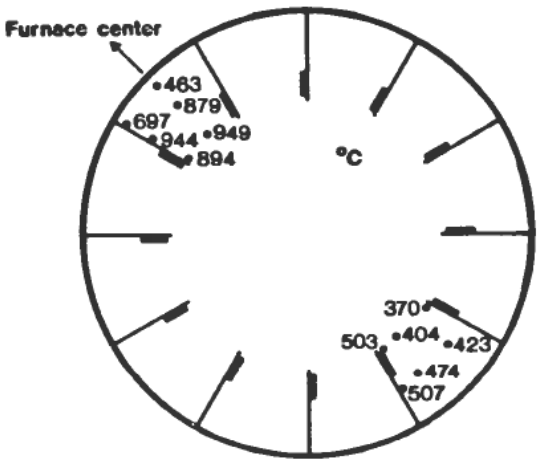

Figure 5. Measured electrode temperatures in a cross-section of the holder.

Three-dimensional calculations make it possible to simulate the problems described above. In this paper we will investigate the effect of some of these parameters.

3. The mathematical model

3.1. General

The model computes the temperature distribution and the electric current distribution in an electrode segment or a complete electrode. A simplified version of a computational domain simulating part of the electrode is shown in Fig. 1.

Electric current is supplied to the electrode in bus tubes and contact clamps. Electric energy is therefore dissipated in the clamps and in the electrode itself. This energy is partly used for the heating and baking of the electrode. The rest is lost through the electrode surface and the water-cooled clamps.

The temperature distribution obviously depends on the electric heat generated by the electric current. The current distribution, on the other hand, is a function of the temperature distribution since the electrical conductivity varies strongly with the temperature. This coupling problem is solved through iteration. The program alternates between computation of the temperature field and the current distribution until convergence is reached.

3.2. Temperature computation

Only the stationary temperature distribution is computed. The electrode slipping is modeled with a mean slip velocity v. The appropriate temperature (T) equation is therefore:

$$\nabla\lambda \,.\, \nabla T + \rho c v \frac{\partial T}{\partial z} + s = 0 \tag{1}$$

where s is the dissipated electric effect, λ is the thermal conductivity, ρ is the density, c is the specific heat capacity and z is the longitudinal (vertical) coordinate.

The computational domain for the temperature equation comprises the electrode and the clamps. The exterior surface of this domain can be fairly complex, and the appropriate boundary conditions have to be specified for each part of this complex surface. Internal boundary conditions (to represent water-cooling in the contact clamps, for instance) are also possible.

3.3. Alternating current computation

For the alternating current computation the pertinent equations are the quasi-stationary approximations of the Maxwell equations. These equations are obtained from the full set of the Maxwell equations by deleting the displacement current term. This means that wave solutions are excluded and that capacitance effects in the electrode are ignored. At the power frequency this is a good approximation. We also assume that Ohm's law is valid and that the magnetic permeability is a constant. Magnetic hysteresis effects are therefore excluded in the model. With these approximations we arrive at a set of equations describing the coupling between the

electric and magnetic fields:

$$\nabla \cdot \mathbf{J} = 0 \tag{2a}$$

$$\nabla \times (\mathbf{J}/\sigma) = -i\omega\mathbf{B} \tag{2b}$$

$$\nabla \cdot \mathbf{B} = 0 \tag{2c}$$

$$\nabla \times (\mathbf{B}/\mu) = \mathbf{J} \tag{2d}$$

where $\mathbf{J}$ is the current density, $\mathbf{B}$ is the magnetic flux density, σ is the electric conductivity, μ is the permeability and ω is the angular frequency of the alternating current. Equations (2a) and (2c) describe the conservation of the electric current and the magnetic flux density. Equation (2b) describes the induction of electric fields by time-varying magnetic fields (Faraday's law), while equation (2d) describes the generation of magnetic fields by electric currents (Ampère's law).

In order to simplify the computation, the magnetic vector potential $\mathbf{A}$ and a scalar potential ϕ are used as primary variables. The current density and the magnetic flux density can then be written as:

$$\mathbf{J} = -\sigma(\nabla\phi + i\omega\mathbf{A}) \tag{3a}$$

$$\mathbf{B} = \nabla \times \mathbf{A} \tag{3b}$$

Equations (2b) and (2c) are then automatically satisfied. We therefore only have to solve for equns (2a) and (2d). These equations can be rewritten as:

$$\nabla\sigma(\nabla\phi + i\omega\mathbf{A}) = 0 \tag{4a}$$

$$\nabla \times \frac{1}{\mu}\nabla \times \mathbf{A} = -\sigma(\nabla\phi + i\omega\mathbf{A}) \tag{4b}$$

To make the computational problem more manageable, the effect of the vertical magnetic field has been ignored. The computational problem is then reduced to solving equn (4a) and the z-component of equn (4b) in the two complex variables ϕ and the vertical A-component.

3.4. Boundary conditions for the current computation

The computational domain for the electric current equations encompasses the whole cylinder sector (dotted outline in Fig. 1). For the air surrounding the electrode, a very low conductivity is used. Boundary conditions must be given both for the current and the magnetic field.

On the boundaries connecting the electrode segment to the rest of the electrode, symmetry conditions are used. On the top and bottom boundary and on the outer cylinder boundary, the magnetic field into the domain is assumed to be zero. The currents are given separately into each bus tube. On the rest of the top boundary and on the outer cylinder boundary, the current into the electrode is zero. On the bottom boundary the currents are assumed to be short-circuited. The program furthermore allows for internal boundary conditions in the form of contact resistance on material boundaries.

3.5. Numerical approximation method

Both the temperature equn (1) and the current equns (4) are discretized in a cylinder (r, θ, z) coordinate system using a finite difference approximation. The computational domain is divided into a three-dimensional array of grid cells by a set of constant coordinate planes. The T- and the ϕ-variables are computed at each grid cell corner. The computational points for the A-variables are displaced half a grid increment in the z-direction as compared to the computational points for the ϕ-variables. By discretizing (1) and (4) we get a set of equations for the T-variables, and another for the A- and the ϕ-variables. The equations are solved iteratively and a rebalancing technique is used to speed up the computation.

A difference method was used in this model instead of a finite element method in order to increase the speed and efficiency of the program. The disadvantage is the limited geometrical flexibility of the difference method. Some details of the electrode, in particular the steel fins, cannot be described properly in a cylinder coordinate system where constant coordinate planes partition the electrode. Therefore, a system for deforming the original cylinder coordinate system, so that the constant coordinate lines coincide with the material boundaries, has been implemented in the program. In this way, a correct steel fin geometry and for instance a gradually smaller electrode radius towards the electrode tip, can be accommodated in the program.

4. Calculations

4.1. General

For computation purposes, the actual domain is divided into several zones: in the radial (r) direction, the tangential (θ) direction and the vertical (z) direction. The zones describe the electrode geometry. They may be subdivided to form a grid of computational points. The basis for a calculation is to compute the heat and current balances for each of these points. A computational domain can be divided into 16 points in the r-, 21 points in the θ- and 11 points in the z-direction, giving a total of 3696 grid points as a maximum number.

The input of the program consists of

geometry description as specified above

temperature dependent material properties

boundary conditions for thermal, electrical and magnetic equations

desired output data

The computer results may be printed out as tables and plots of temperatures, electric current, generated heat and heat flux in various cuts of the electrode. Only temperature plots are presented in this paper.

4.2. Standard case

The model has been used on a series of calculations. A Søderberg electrode with 'normal' operational conditions for FeSi production has been simulated. This calculation, defined as a standard case, has been the reference for other cases where electrode parameters have been changed. Normally, simple changes in one com-

puted case to the next have been performed. We now present some of these cases, emphasizing the practical use of the program.

Case A, the standard case, represents an electrode with a radius of 0·85 m, a current of 130 kA and a slipping rate of 0·6 m/24 h. The boundary conditions are selected from previous two-dimensional calculations. The calculated electrode part covers a geometry similar to the sketch in Fig. 1. The electrode segment is divided into 6 × 10 × 5 zones (=300 zones) and 14 × 15 × 11 gridpoints (=2310 points) in the r-, θ- and z-directions respectively. Furthermore, the segment contains:

1/8 of the electrode cross-section, $\theta = 45°$, ($r = 0{\cdot}85$ m, $z = 6{\cdot}0$ m)

1/8 of the steel casing, 3 mm thick, including 2 fins with reinforcements (out of 16). The fin depth is 300 mm and dimension of the reinforcement 10 × 50 mm.

$2 \times \frac{1}{2}$ contact clamps (out of 8) with 2 copper tubes (out of 16). Each tube conducts 8·125 kA of the electrode current.

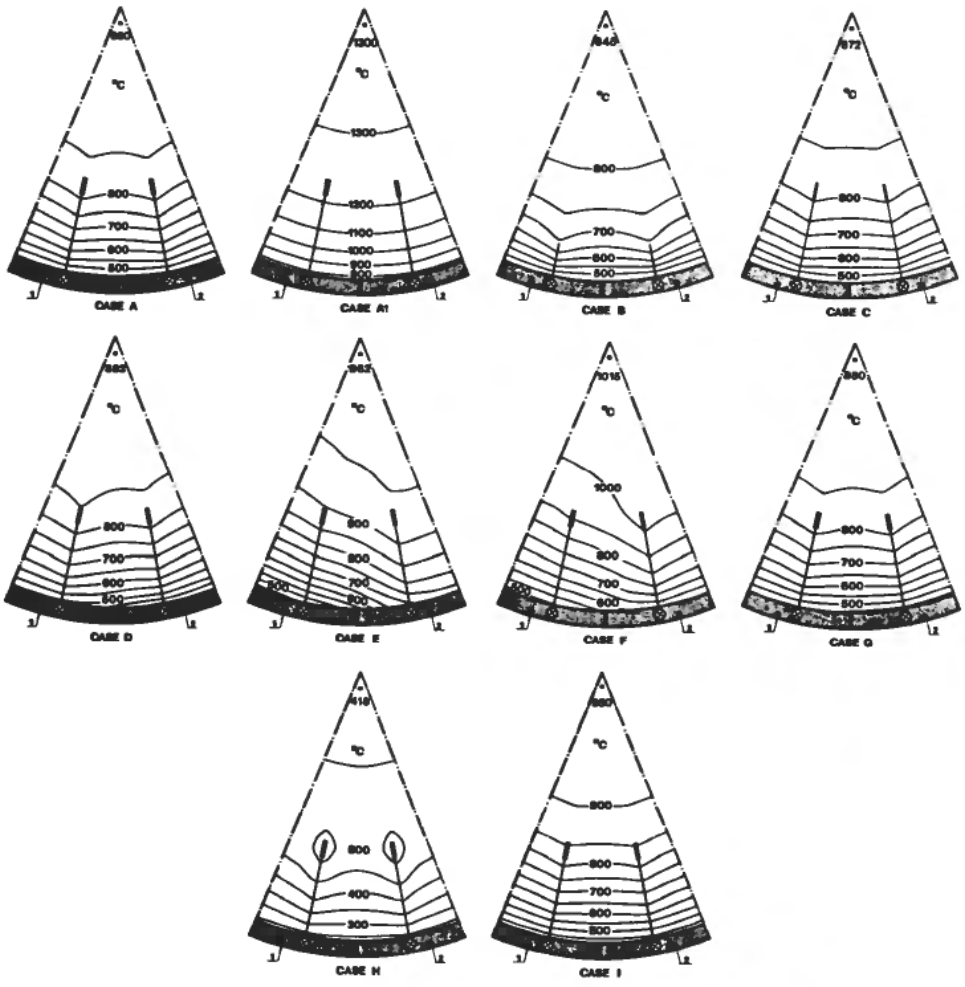

Figure 6. Computed isotherms in cross-sections of the holder.

Case A, Fig. 6, shows isotherms in a cross-sectional area of the calculated segment, selected 0·2 m above the lower end (A), and at the lower end of the contact

clamps (A1). The first illustrates conditions during baking, where the fins are active. Further down in the electrode, at the end of the clamps, a more even temperature distribution is seen. Other parts/levels of the electrode will show different results. Depending on the material composition and the boundary conditions, new temperature and current distributions are found.

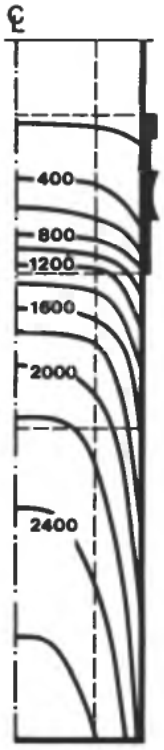

Figure 7. Computed isotherms in the vertical direction.

Figure 7 shows isotherms for the standard case in an *r-z* plane between two fins. These results show good agreement with similar two-dimensional calculations. This is also the case for the electrode heat balance.

4.3. Calculated cases

Case B is changed to an electrode with a short depth of the fins, reduced from 300 mm in Case A to 100 mm, and without reinforcements. No other changes have been introduced compared with the standard. Figure 6 shows different temperatures between the two cases, 0·2 m above the lower end of the clamps. Case B is hottest towards the electrode surface, but shows lower temperatures in the central part.

Case C represents an electrode with stainless steel in the casing. The material properties for steel are changed from case A and the steel sheet in the casing is reduced to 1·5 mm, compared with 3 mm in the standard case. The tensile strength of the two different sheets is approximately the same. The results in Fig. 6 show a somewhat hotter electrode, except in the central part, because of the thin, stainless steel sheet which is used.

Case D is an electrode where two contact clamps with different currents are simulated, 9·75 kA to clamp No. 1 and 6·50 kA to No. 2. The total electrode current is 130 kA as in the other cases. The isotherms in Fig. 6 have been considerably changed compared to the standard, due to an unevenly distributed current.

Case E simulates an electrode where the contact resistances for current transfer between the contact clamps and the electrode casing have been changed. In one of the contact clamps, No. 1, the linear values vary from $2{\cdot}90\ 10^{-4}$ to $1{\cdot}60\ 10^{-5}$ ohm m^2 (standard) at the top and lower holder end, respectively. The other clamp has input from $1{\cdot}45\ 10^{-3}$ to $8{\cdot}00\ 10^{-5}$ ohm m^2. A low resistance means that the current passes further down in the clamps before it enters the electrode. The effect is clearly illustrated in Fig. 6.

Case F is a combination of Cases D and E. The contact resistances are the same as in Case E. A low resistance will tend to transfer more current than one of high resistance. Therefore, the current input is 9·75 kA and 6·50 kA in clamps No. 1 and No. 2, respectively. These adjusted values will give a more correct picture of the current and the temperature distributions. The isotherms are illustrated in Fig. 6.

Case G is a similar computation with different cooling water temperatures in the two contact clamps. In clamp No. 1 the water temperature is reduced to 25°C and in No. 2 increased to 75°C, from the 50°C used in Case A. The relatively small effect is shown in Fig. 6.

Case H demonstrates an increase of the slipping rate from 0·6 m/24 h to 1·2 m/24 h. This is a very high slipping rate even in the production of ferrosilicon, and the position of the baking zone is expected to be too low. The results in Fig. 6 agree with this theory.

Case I is included in the studies in order to demonstrate how the skin effect influences the heat distribution. As mentioned, the standard case is based on alternating current with skin effect. In Case I, however, direct current is supplied to the electrode, giving a much hotter material towards the centre, as illustrated in Fig. 6. The difference seems reasonable.

4.4. New geometry

Case J has been carried out on another geometry, simulating a new concept, the Elkem modular electrode holder, where the current is conducted to the electrode through smaller contact units connected to each of the casing fins. As Fig. 2 shows the fins are extended (Ellefsen 1982) through the steel casing into the contact assembly.

Figure 8 indicates temperature distribution computed at three levels, 0·2 m above the lower end, at the end, and 0·5 m below the lower end of the contact clamps (from left to right). Details cannot be presented in this paper. However, results from the three-dimensional calculations will be an important part of further tests and development.

5. Concluding remarks

Mathematical models are valuable tools in the study of electrode parameters. As already mentioned, our two-dimensional models will take care of the simulations in the vertical and radial directions, as these computations are based on cylindrical geometry. These are relatively inexpensive computations which are easy to perform.

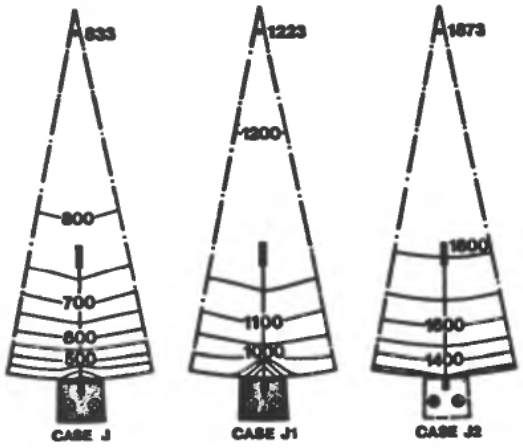

Figure 8. Computed isotherms in cross-sections of the modular holder.

However, if the tangential direction is to be included, as in the simulations described above, only a three-dimensional model is sufficient.

With ELKEM 3X the effect of parameter changes has been studied in Case A through Case I, and the calculation on the modular holder, Case J, has shown the model used on another problem/geometry. Though few results are given in this paper, we have provided some applications of the model. As there are several different values from thousands of calculated points, it is almost impossible to present the complete results. The specific problem to be studied has to be defined before the calculations are carried out and the results presented accordingly.

Mathematical models should be verified with measurements. At present, few such temperatures or other data are available for these simulations. This is due to the measuring technique itself, as well as the possibility to keep stable and defined conditions during the measurements. However, compared with the available data, the results so far seem reasonable. It should also be mentioned that compared with similar two-dimensional computations, which have been verified, the three-dimensional results show good agreement.

The model itself is very complex. Experienced operators with knowledge of electrodes are needed to prepare the input data. Even the results are difficult to present in an understandable form. On the other hand, when the input to a standard case has been worked out, a new calculation for parameter studies is easily performed. Problems with the model application itself are foreseen when working on new, complex constructions.

What is important is that the ELKEM 3X model has proved to be a new tool for treating electrodes more correctly and in more detail than ever before. The most pronounced limit is the number of calculating points, which is closely related to computer time and costs.

This paper demonstrates the application of the model on the important holder area of a Søderberg electrode. The results show that improvements are possible by establishing an even current supply, a uniform cooling and contact pressure for each clamp, and more controlled electrode surroundings. Further work will be performed in cooperation with experts on electrical and mechanical equipment and furnace operations. It is hoped that the results will lead to modifications for improving the electrode.

Acknowledgments

The electrode model has been developed by Elkem a/s and the Institute for Energy Technology. The authors wish to thank the Royal Norwegian Council for Scientific and Industrial Research (NTNF) for financial support.

References

BØCKMAN, O. and OLSEN, L. 1968). Skin and proximity effects in electrodes of large smelting furnaces. No. 127, *6th International Congress of Electroheat*, Brighton.

ELLEFSEN, G. and EVENSEN, K. (1982). Elkem modular electrode holder. ISS/AIME, *40th Electric Furnace Conference*, Kansas City.

INNVAER, R. and OLSEN, L. (1976). Temperatures in Søderberg electrodes in unsteady state conditions. Id No. 5, *8th International Congress of Electroheat*, Liège.

INNVAER, R. and OLSEN, L. (1980). Calculation of thermal stresses in Søderberg electrodes. II Cd 1, *9th International Congress of Electroheat*, Cannes.

OLSEN, L. (1972). Temperature distribution in Søderberg electrodes. No. 405, *7th International Congress of Electroheat*, Warsaw.